



# Crossover-tolerant coated platinum catalysts in hydrogen/bromine redox flow battery

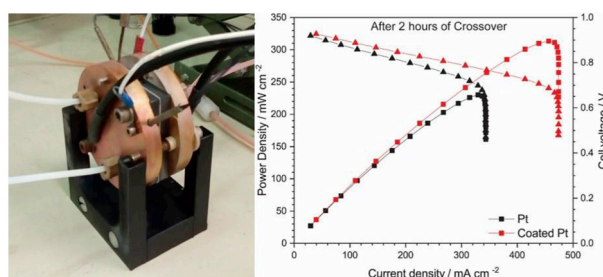
Kobby Saadi, Pilkhaz Nanikashvili, Zhanna Tatus-Portnoy, Samuel Hardisty, Victor Shokhen, Melina Zysler, David Zitoun\*



## HIGHLIGHTS

- High tolerance of the coated catalyst towards bromine crossover.
- High power density of  $550 \text{ mW cm}^{-2}$
- No capacity loss for 100 cycles with the coated catalyst.

## GRAPHICAL ABSTRACT



## ARTICLE INFO

### Keywords:

Electrochemical energy storage  
Redox-flow battery  
Electrocatalysis  
Catalyst  
Nanoparticle  
Bromine

## ABSTRACT

The hydrogen-bromine redox flow battery's ( $\text{H}_2\text{-Br}_2$  RFB) advantages of high energy capacity, high round-trip conversion efficiency and low cost, make it an optimal candidate for large-scale energy storage systems. The crossover of bromide species through the membrane degrades the performance of the  $\text{H}_2\text{-Br}_2$  RFB by poisoning the catalyst responsible for the hydrogen evolution and oxidation reactions. Herein we propose the new concept of a selective catalyst coating layer that mitigates the effect of bromide crossover. The polymerization of dopamine on the catalyst surface yields a nanoscale conformal polydopamine layer which acts as a semi-permeable barrier to block bromide species. The  $\text{H}_2\text{-Br}_2$  RFB with the coated catalyst shows a low capacity fading of 6% at  $300 \text{ mA cm}^{-2}$  after exposure to 4.5 M charged electrolyte for 2 h. Even the beginning of life polarization curves show the benefit of catalyst coating with a high peak power of  $\sim 550 \text{ mW cm}^{-2}$ . Hence, the catalyst coating opens a way to solve the crossover issue in  $\text{H}_2\text{-Br}_2$  RFB technology.

## 1. Introduction

The large interest in renewable energy sources (e.g. solar and wind) during recent years has raised the demand for large-scale, low-cost and durable electrical energy storage (EES) solutions. Although the technology was previously known, Redox Flow Batteries (RFBs) have recently garnered attention as a highly promising choice for EES due to certain advantages over other EES solutions. RFBs are electrochemical energy conversion devices, which exploit redox processes of species in a fluid solution form, stored in external tanks and flowed into the RFB.

High scalability and flexibility, independent sizing of power and energy, high efficiency, long durability and fast responsiveness allow for wide ranges of operational powers and discharge times, which along with a reduced environmental impact makes RFBs ideal for assisting EES from renewable sources [1–3].

The hydrogen-bromine RFB ( $\text{H}_2\text{-Br}_2$  RFB) is one of the most interesting candidates for grid scale EES [4].  $\text{H}_2\text{-Br}_2$  RFB technology displays several unique features such as the high volumetric energy densities of bromine catholyte ( $> 200 \text{ Wh L}^{-1}$ ), the high abundance and low cost of bromine and a high stability of more than 10,000 h

\* Corresponding author.

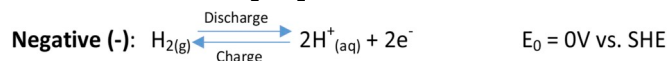
E-mail address: [david.zitoun@biu.ac.il](mailto:david.zitoun@biu.ac.il) (D. Zitoun).

<https://doi.org/10.1016/j.jpowsour.2019.03.043>

Received 13 November 2018; Received in revised form 22 February 2019; Accepted 12 March 2019  
0378-7753/© 2019 Elsevier B.V. All rights reserved.

without significant degradation [5–9].

The reactions in the  $H_2$ – $Br_2$  RFB are:



During charge, the hydro-bromic acid decomposes to  $H_2$ , via the hydrogen evolution reaction (HER), and to  $Br_2$  on a carbonaceous electrode.  $H_2$  can be compressed and stored for use during the discharge cycle. During discharge,  $H_2$  oxidizes to  $H^+$ , via the hydrogen oxidation reaction (HOR), on a catalyst which is currently composed of precious group metals (PGMs). This  $H^+$  combines with bromide species once it has crossed the proton conducting membrane to form the hydro-bromic acid.

The  $H_2$ – $Br_2$  RFB lifetime is mainly limited by the deactivation of the PGM catalyst in the negative electrode [8,10]. The adsorption of bromine and bromide species on the catalyst surface is one of the main reasons for the poisoning of the PGM catalyst and the degradation of the performance in the  $H_2$ – $Br_2$  RFB. The effect of halogen chemisorption on the adsorption of hydrogen, oxygen and methanol on smooth platinum electrodes has been investigated already in the early 1970's [11]. The chemisorption decreases the Pt–H bonding energy and the total amount of adsorption. Early studies have shown the impact of bromide chemisorption on the hydrogen binding energy of Pt single crystals, without decrease of the H coverage [12]. More recent studies show the decrease in the Pt/C electrochemical surface area (ECSA) related to Pt–H desorption by 30% in HBr electrolyte, with major irreversible bromide chemisorption [13]. After washing, Pt can recover only 50% of its initial ECSA. The adsorption of bromides on platinum-group metals is a complex process, which is affected by several factors, including the metal itself and its crystal facets, the concentrations of the bromide species, the type of dosing (from bromine gas or in bromide solution), the pH and the temperature [11].

The main focus of the research in this field dealing with the bromine/bromide crossover and catalyst poisoning was directed at the ability of the membrane to be more selective for bromides without harming its proton conductivity. Membrane-electrode assemblies (MEAs) of  $H_2/Br_2$  RFBs are based on perfluoro-sulfonic acid (PFSA) membranes such as Nafion®. PFSA membranes should selectively transport protons while blocking  $H_2$  and bromine/bromides species. Reducing Nafion concentration in membranes decreases the conductivity and the permeability of the membrane [14]. Membrane conductivity limits system efficiency at high current density, and the bromine/bromide crossover limits efficiency at low current density. The performance and the efficiency of the cell are more sensitive to membrane thickness and pretreatment procedure than the equivalent weight and the reinforcement of the membrane. After more than 3000 h of operating a cell with pretreated membrane, the bromine crossover decreased moderately, but remained higher than the crossover of the as-received membrane [9]. Tucker et al. illustrates the competition between adsorbed hydrogen and bromide ions on the Pt surface by testing the electrode potential response to hydrogen shortage and  $Br_2/HBr$  contamination. Bromide reversibly adsorbs at the hydrogen electrode when its potential exceeds a critical value, resulting in a peak limiting cell current [15,16]. Other types of membranes such as nanoporous proton conducting membranes (NP-PCM) made of polyvinylidene fluoride (PVDF) and silica are even more prone to  $Br_2/HBr$  crossover with a high liquid flux across the NP-PCM membrane [17].

Since no membrane can completely block crossover, the investigation of poisoning/corrosion tolerant catalysts is of major importance.

Pt-rich alloys show a better tolerance to bromide poisoning [9]. Rhodium sulfide catalysts demonstrates high tolerance but low initial catalytic activity [18,19]. Other ternary sulfides of earth abundant transition metals and Ru ( $Co_{0.3}Ru_{0.7}S_2$ ) show interesting HER activity in HBr but are inactive towards HOR [20]. Therefore, the main path towards crossover tolerance goes through the investigation of Pt-rich catalysts, as shown with the successful development of a bromide tolerant Pt–Ir– $N_x$ /C catalysts [21].

In a recent study we have shown that a nanoscale polydopamine coating on a Pt catalyst can effectively protect the catalyst surface from corrosion in 3 M HBr, allowing the catalyst to maintain its activity (when measured via a rotating disc electrode) [22]. The catalytic activity of the polydopamine coated Pt remains high, even after dipping the catalyst in concentrated HBr for hours, with an almost unchanged hydrogen diffusion constant. Herein, we implement the use of polydopamine coated Pt in a  $H_2$ – $Br_2$  RFB in an effort to prevent Pt poisoning during the unavoidable bromine crossover. Upon  $H_2$  pressure release, charged electrolyte rapidly crosses through the nanoporous proton conducting membranes (NP-PCM). The  $H_2$ – $Br_2$  RFB with polydopamine coated Pt catalyst shows a low capacity fading of 6% at  $300 \text{ mA cm}^{-2}$  after exposure to 4.5 M charged electrolyte for 2 h. Even the beginning of life polarization curves shows the benefit of catalyst coating with a high peak power of  $\sim 550 \text{ mW cm}^{-2}$ .

## 2. Experimental

### 2.1. Catalyst synthesis

The Pt catalyst polydopamine coating has been described in a recent publication [22]. The polymer coating was conducted on a standard Pt black catalyst (Premetek). The dopamine was polymerized in an aqueous dispersion of the catalyst (5 mg/mL) from dopamine hydrochloride (Sigma Aldrich, 99%) in tris-HCl pH 7.5 buffer solution (10 mmol/L - Tris-HCl Trizma base, Sigma Aldrich) under magnetic stirring in a glass vial for 20 min at 25 °C. At the end of the reaction, the residual dopamine was washed from the sample three times with absolute ethanol and deionized water by sequential centrifugation/dispersion procedures. Afterwards, the catalyst was dried in a vacuum oven at 80 °C for 4 h. After the polydopamine coating, we performed thermal annealing of the sample at 150 °C for 60 min under  $N_2$ . The structure was investigated by Transmission Electron Microscopy (TEM) on a JEOL 1400 (LaB<sub>6</sub>) operating at 200 kV.

### 2.2. Preparation of catalyst inks and fabrication of MEAs

Both electrodes were supported on SGL 29AA carbon paper. All the wet layers were coated via a Doctor Blade coater. The bromine electrode contains one layer of PVDF (Kynar 2801, Arkema), carbon black Vulcan (XC72R, Cabot), Pt catalyst powder ( $\sim 0.01 \text{ mg cm}^{-2}$ ) and a pore former (Propylene Carbonate, Sigma-Aldrich). The hydrogen electrode was made from two layers of carbon black and PVDF. The catalytic ink was a dispersion of the coated Pt catalyst, carbon black and high surface area graphite (HSAG 300, Timcal) in water, 2-propanol, TBAOH (tetrabutyl ammonium hydroxide in Methanol 1 M, Sigma-Aldrich) and 5% Nafion solution mixture. It was mixed overnight before thin coating. After drying and Nafion curing for 1 h at 145 °C, the electrode was washed for 1 h at 80 °C in 0.5 M  $H_2SO_4$  and for 1 h at 80 °C in water and was then dried at 100 °C. The top layer of the electrode was applied via spraying with 5% Nafion solution mixture (50% in Ethanol). After drying under ambient conditions and Nafion curing (1 h at 145 °C), the electrode was ready for the MEA.  $7 \text{ cm}^2$  electrodes in Teflon frames were hot pressed (100 °C for 45 s) to the membrane (NP-PCM,  $\sim 200 \mu\text{m}$ ) [23,24]. The Teflon frames (100  $\mu\text{m}$  for the bromine electrode and 200  $\mu\text{m}$  for hydrogen electrode) are to keep the electrode's thickness and for sealing the cell. The MEA was located between two graphite plates which were tightened between two

copper current collectors. The flow channels of the solution side are interdigitated and the gas side is single serpentine.

### 2.3. RFB operation

Cells were operated with dry hydrogen and 20 ml recycled 4.5 M HBr solution ( $12 \text{ ml min}^{-1}$ ) at  $40^\circ\text{C}$ . Hydrogen pressure was controlled by a needle valve on the cell exhaust line. Polarization curves and cycling tests were obtained using a Biologic Science Instruments BCS-815 battery cycler.

The initial step of each cell was a deep charging to 60% SOC. After AC measurement, micro and macro polarization tests were operated. After discharge and another AC measurement, voltage limits were obtained and the cell started its cycling. After more than 100 cycles, and in order to test the catalyst in strict conditions, the hydrogen flow was stopped for 30 min and for 2 h. Following every hydrogen stop, a polarization test made to compare the ability of the coated and un-coated catalyst to recover after hydrogen stoppage.

### 2.4. Electrochemical, structural and chemical diagnostics

The electrochemical surface area (ECSA) of new electrodes was measured via cyclic voltammetry (CV) and was compared to the ECSA of the electrodes after soaking for 2 h in hydrobromic acid (HBr 4.5 M). The electrolyte of all the measurements was perchloric acid ( $\text{HClO}_4$ , 0.1 M). After a purge of Ar for 10 min, the voltammogram was collected at scan rate of  $20 \text{ mV/s}$ , from 0 V to 0.8 V vs. standard hydrogen reference electrode and with a platinum wire as a counter electrode. All the data was collected on the impedance channel of the potentiostat (Bio-Logic VMP3). The potentials were corrected for ohmic loss by measuring impedance before every polarization curve (iR free measurement). The ECSA was calculated from the  $\text{H}_{\text{UPD}}$  between 0.015 and 0.25 V.

The used electrodes were investigated by High Resolution Scanning Electron Microscopy (HR-SEM) FEI, Magellan 400 L in order to compare the exposure of both electrodes to bromine species. Samples of new and used electrodes were investigated with X-ray Photoelectron Spectroscopy (XPS) in order to better understand the surface structure of the first nanometric layers of the electrodes that are closest to the membrane and determine the electrode performance in the cell. The XPS analysis was carried out using Kratos Axis HS spectrometer (England) equipped with a monochromatic Al K $\alpha$  X-ray source (photon energy 1486.6 eV).

The quantity of platinum on both electrodes was measured by X-ray fluorescence (XRF) using a XGT 7200 from Horiba to compare new and used electrodes. The tested point diameter was  $10 \mu\text{m}$  and the pixel width was  $6 \mu\text{m}$ .

## 3. Results and discussion

In this work, we focus on a catalyst coating to mitigate Pt catalyst deactivation. The catalyst coating is adopted from our previous work where the polydopamine nanoscale film on Pt catalyst shows high selectivity to hydrogen species and blocks bromide species [22]. Impeding bromide chemisorption improves the durability of Pt catalyst in 3 M HBr.

Herein, the polydopamine coated Pt serves as hydrogen catalyst in a  $\text{H}_2\text{-Br}_2$  RFB. The overall design of the cell is described in the experimental section. The use of a PVDF thick membrane is primordial to achieve a low cost and long lifetime EES.

The negative electrode is coated with a Pt loading of  $0.95 \pm 0.1 \text{ mg cm}^{-2}$ . The  $\text{H}_2\text{-Br}_2$  RFB is run at  $40^\circ\text{C}$  with an initial HBr concentration of 4.5 M. At beginning of life, the standard Pt catalyst layer shows an OCV of 0.95 V, close to the thermodynamic potential of the cell. The polarization curve shows a peak power of  $480 \text{ mW cm}^{-2}$  with a potential of 0.8 V at  $300 \text{ mA cm}^{-2}$  (Fig. 1). These

values match the needs for EES.

Compared to standard Pt, the coated Pt electrode displays an increase of 14% in peak power density and 2.5% in voltage at  $300 \text{ mA cm}^{-2}$  discharge. The initial micro-polarization resistors of the coated platinum cell are lower by 26% than those of the plan platinum cell ( $0.45 \Omega \text{ cm}^2$  vs.  $0.61 \Omega \text{ cm}^2$ ). We did not expect the higher peak power measured for the coated Pt electrode since we expect the ECSA to be reduced by the coating (as will be confirmed below). At this stage, the main explanation for the higher peak power observed for the coated catalyst would be the bromine crossover taking place even at this very early stage, which we call beginning of life. In fact, the initial micro-polarization occurs several hours after the cell assembly and exposure to the electrolyte.

Those resistors grow during the operation of the cells at a similar rate. The lower impedance of the cell is related to the interface between the Pt catalyst and the electrolyte. In our previous study, we have shown that a Pt catalyst undergoes chemisorption processes which account for the large variations of impedance. On the contrary, coated Pt catalysts have a lower impedance and are stable over time, even in a bromide environment [22].

Long-term galvanostatic cycling of the RFB is compared for the two catalyst layers (Fig. 2). The capacity shows a constant fading and the initial capacity can be fully restored (and even improved) with a fresh electrolyte. The sharp steps in the galvanostatic cycling correspond to the refilling of a fresh electrolyte. This phenomenon is inherent to the testing procedure used in the laboratory, where the electrolyte container is not fully sealed. The charge capacity of both cells is almost similar (at approx. 1100 mAh for a  $7 \text{ cm}^2$  cell), but the operational voltage window of the coated catalyst layer is narrower by 0.1 V than the pristine Pt catalyst layer. Narrowing the operational voltage window can certainly enable a better durability of the coated catalyst, since platinum poisoning occurs mainly at high overpotential on the negative electrode [22]. The coated Pt cell reaches better efficiencies, with an overall energy efficiency (EE) of 72% (coulombic efficiency CE:89%, voltage efficiency VE:81%) compared to the plain Pt cell (EE:68%, CE:90%, VE:76%). The enhancement in peak power density and overall EE is related to the decrease of the impedance with polydopamine Pt catalyst coating. This result may appear rather counter-intuitive, since a polymeric layer should increase the contact resistance at the catalyst surface, but it's consistent with the formation of a stable interface with high hydrogen diffusion constants.

The polarization curves after cycling show the main discrepancy between the coated Pt catalyst and the pristine Pt catalyst (Fig. 2C and D). While the pristine Pt catalyst displays a significant decrease of the peak power density (25% loss at cycle 51), the coated Pt catalyst does not suffer from any capacity loss, even after 90 cycles. The peak power density slightly increases with the addition of a fresh electrolyte. This striking result reflects the deactivation of the Pt catalyst at work in the gas diffusion electrode. As pointed in the introduction, the proton conducting membrane is not fully selective and bromine crossover occurs during the cell operation.

After a few days of stable operation, the catalyst layer faced its first significant challenge when the hydrogen flow was stopped for 30 min on the anode. The hydrogen shortage is a practical accelerated stress test to force the bromine crossover through the membrane. The OCV rapidly drops to less than 10 mV and the Pt catalyst layer is flooded with charged electrolyte (4.5 M solution). The orange color of the  $\text{Br}_3^-$  ions was easily observed even in the hydrogen pipes.

After restarting and stabilizing the hydrogen flow and the OCV, a polarization test was conducted. As shown in Figs. 3A and 4A and Table 1, both cells performances decrease but the voltage of the coated platinum cell at  $300 \text{ mA/cm}^2$  is still 2.2% higher than the uncoated Pt cell. The coated Pt cell still has better efficiencies (CE:90%, EE:71%, VE:79%) compared to the uncoated Pt cell (CE:90%, EE:69%, VE:77%).

After three days of continuous operation of the cells in charge/discharge mode, they face an even greater challenge: hydrogen flow

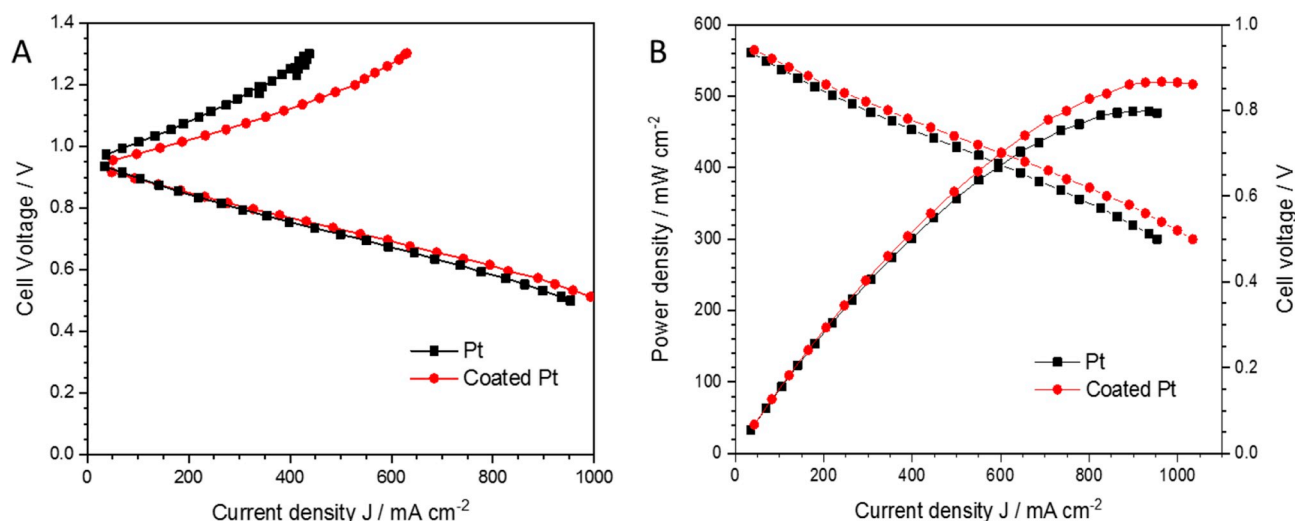


**Fig. 1.** Initial Polarization curves of H<sub>2</sub>–Br<sub>2</sub> RFB with GDE made of Pt (black squares) or coated Pt (red dots): (A) charge/discharge; (B) discharge and power density. (For interpretation of the references to color in this figure legend, the reader is referred to the Web version of this article.)

stoppage for 2 h. As in the first hydrogen stop, the OCV drops to few millivolts after 12 min. During this long break, the OCV reaches almost 0 V which means that there is no hydrogen left in the negative electrode to protect the catalyst from chemisorption of bromine species which floods the membrane and the negative electrode. The hydrogen

electrode is totally flooded with a 4.5 M charged solution. This accelerated stress test is the most extreme case of catalyst deactivation. When the hydrogen flow restarts, the orange colored electrolyte is drawn out of the exhaust line. The recovery from this case is longer than before. After cycling at low discharge current (100 mA cm<sup>-2</sup>)

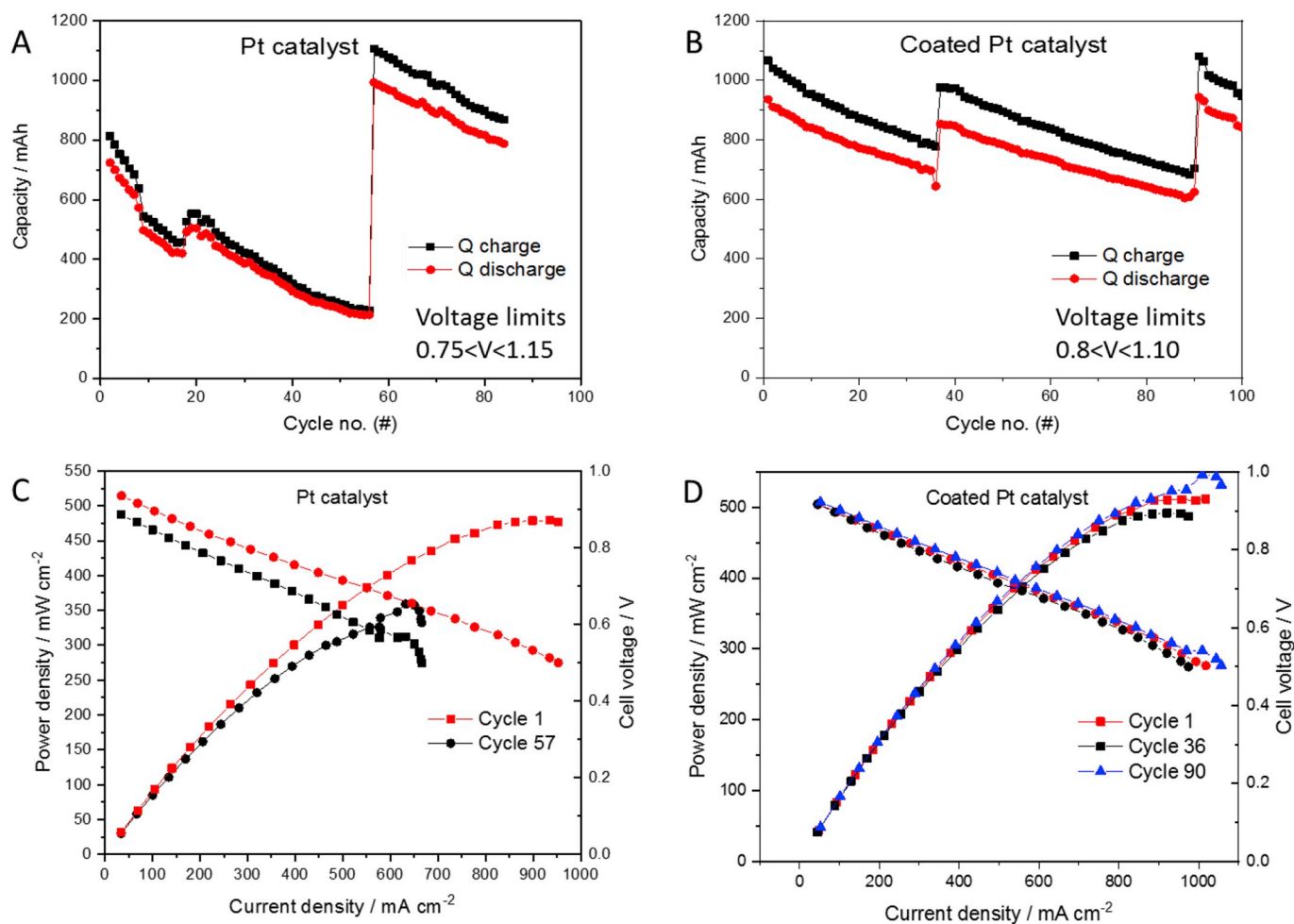


**Fig. 2.** Cycling of H<sub>2</sub>–Br<sub>2</sub> RFB with gas diffusion electrode (GDE) made of (A) platinum catalyst and (B) polydopamine coated platinum catalyst. Polarization curves after addition of fresh electrolyte for Pt GDE (C) and coated Pt GDE H<sub>2</sub>–Br<sub>2</sub> RFB (D).

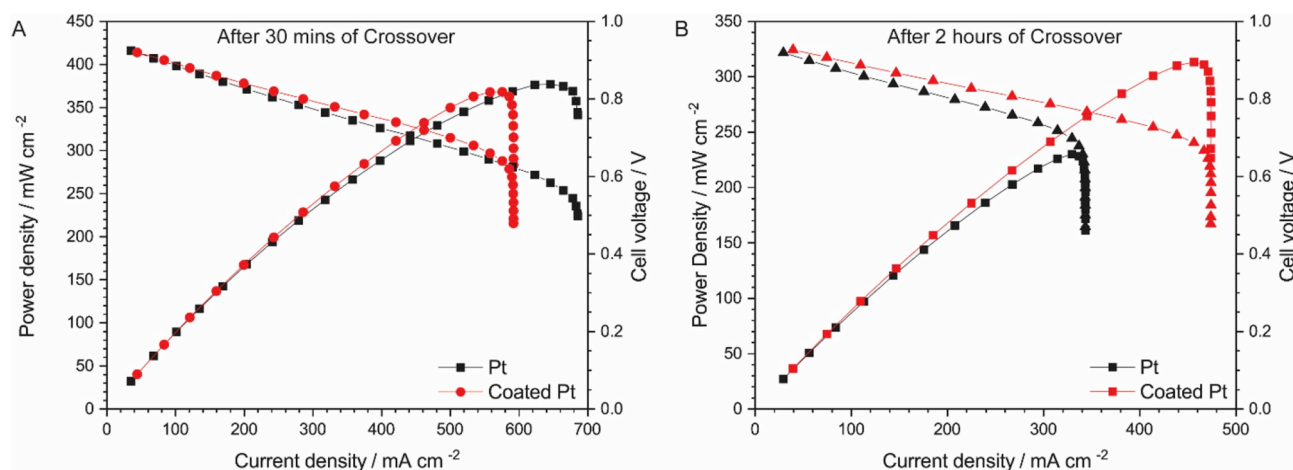


**Fig. 3.** Polarization curves of  $H_2$ – $Br_2$  RFB with GDE made of Pt (black squares) or coated Pt (red dots) (A); after 30 min of hydrogen shortage and (B); after 2 h of hydrogen shortage. (For interpretation of the references to color in this figure legend, the reader is referred to the Web version of this article.)

overnight, we run a polarization test. The comparison is shown in Figs. 3B and 4B and Table 1. The difference between the cells now is more significant. The power density peak of the cell with the coated Pt catalyst is 17.4% higher than the pristine Pt catalyst and the cell voltage at  $300\text{ mA cm}^{-2}$  is 4.9% higher. The coated platinum cell has better voltage efficiency (79%) than the platinum cell (74%). Even after 2 h hydrogen shortage, the coated Pt cell's impedance is significantly lower than the uncoated Pt cell ( $0.57\ \Omega\text{ cm}^2$  vs.  $0.75\ \Omega\text{ cm}^2$ ).

The electrochemical surface area (ECSA) of the gas diffusion electrodes is calculated from the hydrogen desorption charge on the cyclic voltammetry (CV) measurements in  $0.1\text{ M HClO}_4$  before and after soaking for 2 h in  $4.5\text{ M HBr}$  (Fig. 5). The results are summarized in Table 2. Pristine Pt black shows the typical adsorption/desorption hydrogen features corresponding to the crystallographic facets of Pt ( $\{110\}$  and  $\{200\}$ ). These features disappear after soaking in HBr. On the coated platinum electrode, the polymeric coating on the catalyst powder broadens the hydrogen adsorption/desorption region. The coated Pt electrode has a remarkably stable ECSA after soaking in HBr. The coated Pt ECSA decreases by only 5%, while the pristine Pt ECSA decreases by 30%. This immunity towards Br poisoning/corrosion is consistent with our previous measurements on rotating disc electrodes [22].

To further prove the bromine crossover and to assess the surface

**Table 1**

Power density peak and cell voltage comparison of the two cells after hydrogen shortage.

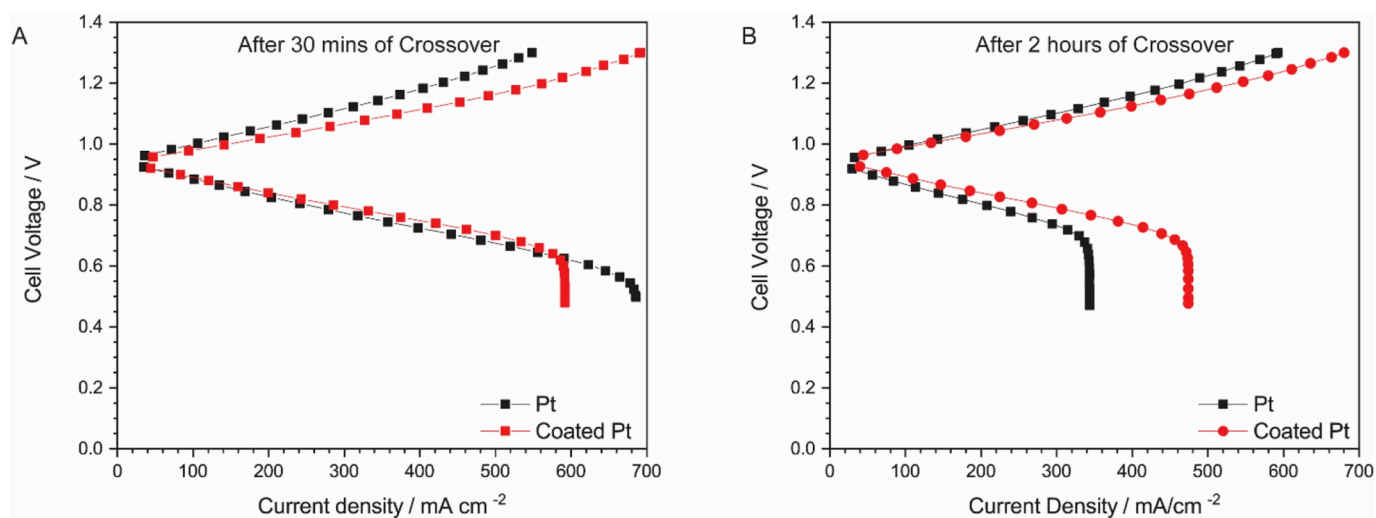
		Peak Power Density [ $\text{mW}/\text{cm}^2$ ]			
		New	After (#) cycles	30 min. $H_2$ stop	2 h $H_2$ stop
Pt		479	(#57) 359	377	230
Coated Pt		520	(#90) 546	368	270

		Cell voltage at $300\text{ mA}/\text{cm}^2$ [mV]			
		New	After (#) cycles	30 min. $H_2$ stop	2 h $H_2$ stop
Pt		798	(#57) 730	777	732
Coated Pt		807	(#90) 818	794	768

state of the catalysts after crossover, a series of post-mortem experiments were carried out on the gas diffusion electrodes (GDE). After the cells are disassembled, the used hydrogen GDEs are peeled from the membrane and observed by HR-SEM (Fig. 6). The elemental mappings from EDAX show the large amount of bromine species in both electrodes, which remain even after further cycling and proper washing of the GDEs.

The XRF semi-quantitatively measures the amount of platinum in the electrode before and after exposure to bromide species (as discussed



**Fig. 4.** Charge/discharge polarization curves of  $H_2$ – $Br_2$  RFB with GDE made of Pt (black squares) or coated Pt (red dots) (A); after 30 min of hydrogen shortage, (B); and after 2 h of hydrogen shortage. (For interpretation of the references to color in this figure legend, the reader is referred to the Web version of this article.)

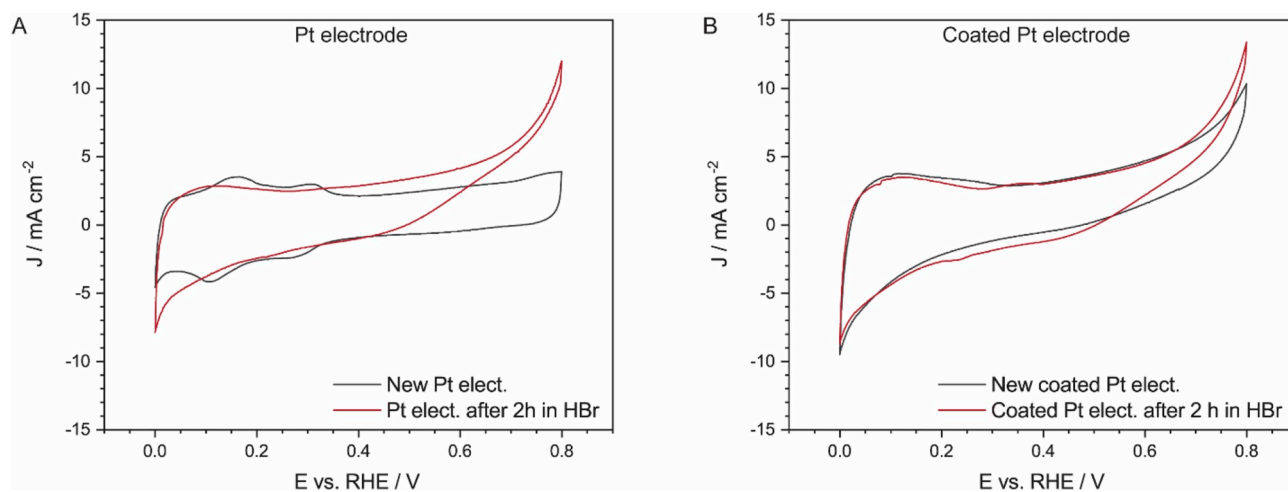


**Fig. 5.** Cyclic Voltammetry (CV) of (A); platinum and (B); coated platinum electrodes, before (black line) and after (red line) soaking in HBr. (For interpretation of the references to color in this figure legend, the reader is referred to the Web version of this article.)

**Table 2**

Electrode's ECSA comparison before and after exposure to 4.5 M HBr.

	ECSA – new electrode (m <sup>2</sup> /g)	ECSA after 2 h in 4.5 M HBr (m <sup>2</sup> /g)
Pt electrode	22.9	15.5
Coated Pt electrode	20.5	19.4

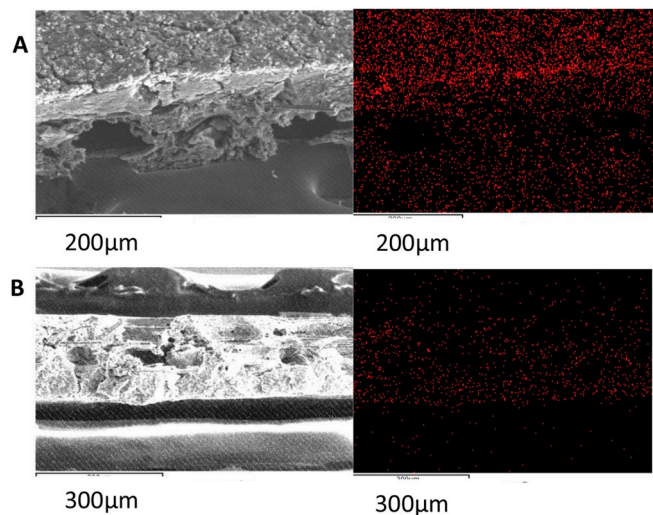


**Fig. 6.** HR-SEM cross section images and EDS mapping of bromide for used electrodes with (A); plan platinum (B); and coated platinum.

above) and further operation of the RFB (Fig. 7). For beginning of life GDE, with pristine and coated Pt, the XRF spectrum reveals the same amount of Pt, consistent with the Pt loading ( $0.95 \pm 0.1 \text{ mg cm}^{-2}$ ). The post-mortem GDEs show a large discrepancy in the Pt content. The XRF spectrum of the Pt catalyst without coating does not display the Pt L lines anymore while the coated catalyst still shows the Pt L lines, albeit with a lower intensity. Further experiments are needed to quantitatively measure the Pt content in the GDEs after cell operation. In any case, the significant loss of platinum in the electrode can explain the performance fading.

X-ray photoelectron spectroscopy (XPS) gives a more precise

knowledge on the surface state of the catalysts and reflects the chemical nature of the catalysts surface in the gas diffusion electrodes, before and after crossover and cycling of the RFB (Fig. 8). The coated and pristine Pt catalysts display a similar XPS spectrum and the Pt 4f lines can be fitted with two components corresponding to the Pt(0) and Pt(II) oxidation states. After exposure to bromide species, the XPS of the pristine Pt does not show any noticeable lines. It may indicate that exposure to bromine creates a film on the surface of the pristine Pt catalyst and/or corrodes the unprotected Pt. The formation of a surface film on the Pt catalyst surface is consistent with the decrease of the ECSA. On the other hand, the exposure to bromine does not alter the XPS spectrum of coated Pt. It proves that the polydopamine coating contributes to the Pt chemical stability even after long exposure to bromine species, in conditions where uncoated Pt catalyst undergoes deactivation following a chemisorption and corrosion process.

#### 4. Conclusions

Catalyst poisoning on the hydrogen electrode of H<sub>2</sub>–Br<sub>2</sub> RFB is one of the critical issues that affects its performance and durability. Herein, we have synthesized a polydopamine nanoscale coating on a standard Pt catalyst. The peak power density of the polydopamine coated Pt catalyst is 14% higher than uncoated Pt, reaching  $550 \text{ mW cm}^{-2}$ , with lower values of impedance and higher energy efficiency. The voltage of the H<sub>2</sub>–Br<sub>2</sub> RFB cell during cycling is higher for the coated catalyst at the beginning of life. After three days of cycling, the H<sub>2</sub>–Br<sub>2</sub> RFB with a coated catalyst does not show any sign of capacity fading, compared to the 25% losses observed with the pristine Pt catalyst. After long exposure to charged electrolyte (4.5 M at 40 °C) on the negative electrode, the H<sub>2</sub>–Br<sub>2</sub> RFB with a coated catalyst shows an increase in peak power density of 17% and lower values of impedance compared to uncoated Pt catalyst. Advanced electrochemical and spectroscopic investigations of the used hydrogen gas diffusion electrodes show the stability of the electrochemical surface area for the coated catalysts, compared to the uncoated catalyst. The polydopamine coating effectively stabilizes the surface of the catalyst and acts as an efficient barrier against bromine chemisorption and corrosion. The coated catalyst shows no sign of deactivation even during the accelerated stress test, offering a practical solution to one of the main bottlenecks in the way to energy efficient H<sub>2</sub>–Br<sub>2</sub> RFB.

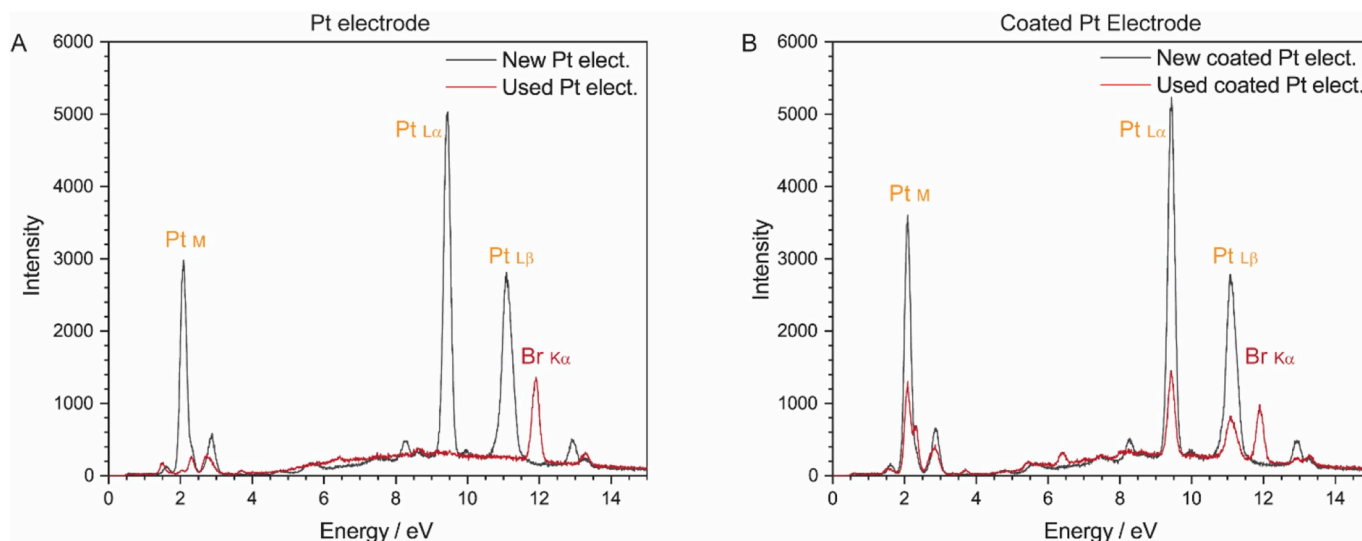


Fig. 7. XRF spectra on the gas diffusion electrode after crossover and cycling for: (A) pristine platinum and, (B) coated platinum.

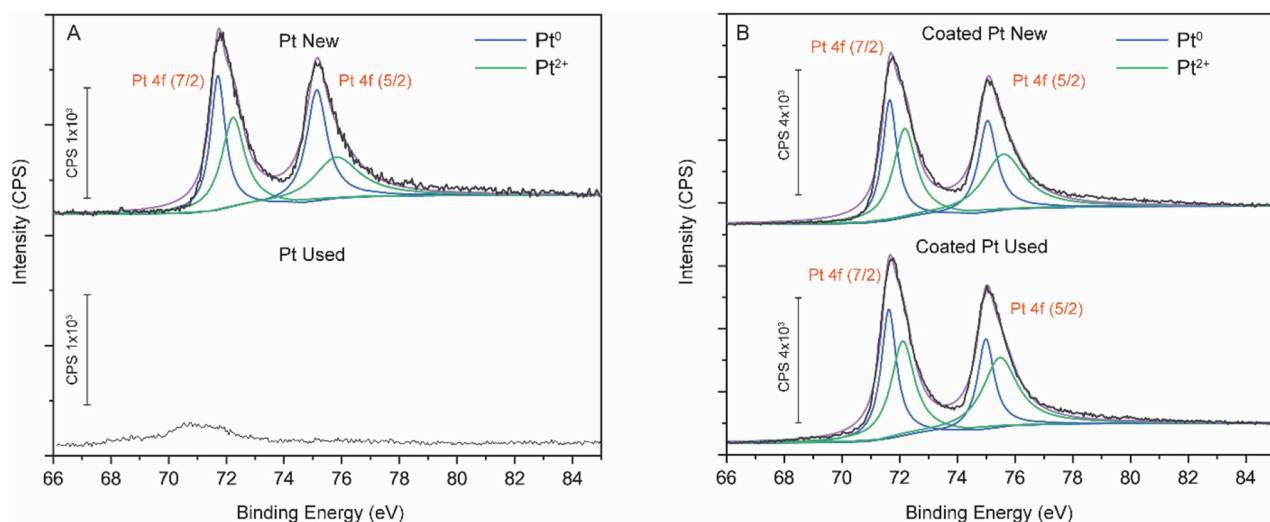


Fig. 8. XPS results for (A); plan platinum (B); and coated platinum.

## Declarations of interest

None.

## Acknowledgments

The authors are grateful to the Israel Ministry of Science and Technology (MOST) for financial support of the project through the German-Israeli Battery and Electrochemistry Research Program. S.H. acknowledges the Horizon 2020 Flowcamp ITN for his financial support. The authors acknowledge Dr. Michal Ejgenberg for her kind assistance with XPS.

## References

- [1] P. Alotto, M. Guarnieri, F. Moro, Redox flow batteries for the storage of renewable energy: a review, *Renew. Sustain. Energy Rev.* 29 (2014) 325–335, <https://doi.org/10.1016/j.rser.2013.08.001>.
- [2] G.L. Soloveichik, Flow batteries: current status and trends, *Chem. Rev.* 115 (2015) 11533–11558, <https://doi.org/10.1021/cr500720t>.
- [3] J. Noack, N. Roznyatovskaya, T. Herr, P. Fischer, The chemistry of redox-flow batteries, *Angew. Chem. Int. Ed.* 54 (2015) 9776–9809, <https://doi.org/10.1002/anie.201410823>.
- [4] E. Knudsen, P. Albertus, K.T. Cho, A.Z. Weber, A. Kojic, Flow simulation and analysis of high-power flow batteries, *J. Power Sources* 299 (2015) 617–628, <https://doi.org/10.1016/j.jpowsour.2015.08.041>.
- [5] R.S. Yeo, J. McBeen, Transport properties of nafion membranes in electrochemically regenerative hydrogen/halogen cells, *J. Electrochem. Soc.* 126 (1979) 1682–1687, <https://doi.org/10.1149/1.2128776>.
- [6] R. Yeo, D.-T. Chin, A hydrogen-bromine cell for energy storage applications, *J. Electrochem. Soc.* 21 (1982) 3335–3338, <https://doi.org/10.1117/12.771968>.
- [7] G.G. Barna, Oxidation of H<sub>2</sub> at gas diffusion electrodes in H<sub>2</sub>SO<sub>4</sub> and HBr, *J. Electrochem. Soc.* 129 (1982) 2464, <https://doi.org/10.1149/1.2123568>.
- [8] G.G. Barna, S.N. Frank, T.H. Teherani, L.D. Weedon, Lifetime studies in H<sub>2</sub>/Br<sub>2</sub> fuel cells, *J. Electrochem. Soc.* 131 (1984) 1973–1980.
- [9] J.A. Kosek, A.B. Laconti, Advanced hydrogen electrode for a hydrogen-bromine battery, *J. Power Sources* 22 (1988) 293–300, [https://doi.org/10.1016/0378-7753\(88\)80024-7](https://doi.org/10.1016/0378-7753(88)80024-7).
- [10] K.T. Cho, M.C. Tucker, A.Z. Weber, A review of hydrogen/halogen flow cells, *Energy Technol.* 4 (2016) 655–678, <https://doi.org/10.1002/ente.201500449>.
- [11] V.S. Bagotzky, Y.B. Vassilyev, J. Weber, J.N. Pirtskhalava, Adsorption of anions on smooth platinum electrodes, *J. Electroanal. Chem.* 27 (1970) 31–46, [https://doi.org/10.1016/S0022-0728\(70\)80200-5](https://doi.org/10.1016/S0022-0728(70)80200-5).
- [12] N.M. Markovic, C.A. Lucas, H.A. Gasteiger, P.N. Ross, Bromide adsorption on Pt (100): rotating ring-Pt(100) disk electrode and surface X-ray scattering measurements, *Surf. Sci.* 365 (1995) 229–240, [https://doi.org/10.1016/S0049-237X\(06\)80050-9](https://doi.org/10.1016/S0049-237X(06)80050-9).
- [13] M. Goor-Dar, N. Travitsky, E. Peled, Study of hydrogen redox reactions on platinum nanoparticles in concentrated HBr solutions, *J. Power Sources* 197 (2012) 111–115, <https://doi.org/10.1016/j.jpowsour.2011.09.044>.
- [14] J.W. Park, R. Wycisk, P.N. Pintauro, Membranes for a regenerative H<sub>2</sub>/Br<sub>2</sub> fuel cell, *ECS Trans* 50 (2013) 1217–1231.
- [15] M.C. Tucker, K.T. Cho, F.B. Spingler, A.Z. Weber, G. Lin, Impact of membrane

- characteristics on the performance and cycling of the Br<sub>2</sub>-H<sub>2</sub>redox flow cell, *J. Power Sources* 284 (2015) 212–221, <https://doi.org/10.1016/j.jpowsour.2015.03.010>.
- [16] M.C. Tucker, K.T. Cho, A.Z. Weber, G. Lin, T. Van Nguyen, Optimization of electrode characteristics for the Br<sub>2</sub>/H<sub>2</sub> redox flow cell, *J. Appl. Electrochem.* 45 (2015) 11–19, <https://doi.org/10.1007/s10800-014-0772-1>.
- [17] V. Livshits, A. Ulus, E. Peled, High-power H<sub>2</sub>/Br<sub>2</sub> fuel cell, *Electrochem. Commun.* 8 (2006) 1358–1362, <https://doi.org/10.1016/j.elecom.2006.06.021>.
- [18] J. Masud, T. Van Nguyen, N. Singh, E. McFarland, M. Ikenberry, K. Hohn, C.-J. Pan, B.-J. Hwang, A RhxSy/C catalyst for the hydrogen oxidation and hydrogen evolution reactions in HBr, *J. Electrochem. Soc.* 162 (2015), <https://doi.org/10.1149/2.0901504jes> F455–F462.
- [19] V. Yarlagadda, R.P. Dowd, J.W. Park, P.N. Pintauro, T. Van Nguyen, A comprehensive study of an acid-based reversible H<sub>2</sub>-Br<sub>2</sub> fuel cell system, *J. Electrochem. Soc.* 162 (2015), <https://doi.org/10.1149/2.1041508jes> F919–F926.
- [20] A. Ivanovskaya, N. Singh, R.F. Liu, H. Kreutzer, J. Baltrusaitis, T. Van Nguyen, H. Metiu, E. McFarland, Transition metal sulfide hydrogen evolution catalysts for hydrobromic acid electrolysis, *Langmuir* 29 (2013) 480–492, <https://doi.org/10.1021/la3032489>.
- [21] G. Lin, P.Y. Chong, V. Yarlagadda, T. V Nguyen, R.J. Wycisk, P.N. Pintauro, M. Bates, S. Mukerjee, M.C. Tucker, A.Z. Weber, Advanced hydrogen-bromine flow batteries with improved efficiency, durability and cost, *J. Electrochem. Soc.* 163 (2016) A5049–A5056, <https://doi.org/10.1149/2.0071601jes>.
- [22] G. Gershinsky, P. Nanikashvili, R. Elazari, D. Zitoun, From the sea to hydrobromic acid: polydopamine layer as corrosion protective layer on platinum electrocatalyst, *ACS Appl. Energy Mater.* 1 (2018) 4678–4685, <https://doi.org/10.1021/acsaem.8b00808>.
- [23] E. Peled, A. Blum, US patent number 8,968,961 B2.
- [24] E. Peled, A. Blum, A. Aharon, Y. Konra, V. Zel, K. Saadi, US patent number 9,012,104 B2.